Relaxation properties of rare-earth ions in sulfide glasses: Experiment and theory

V. G. Truong,[1,2] B. S. Ham,[2,*] A. M. Jurdyc,[1] B. Jacquier,[1] J. Leperson,[3] V. Nazabal,[3] and J. L. Adam[3]
[1]*Laboratoire de Phisico-Chimie des Materiaux Luminescents, UMR-CNRS 5620, Universite de Lyon 1, Domaine Scientifique de la Doua, 69622 Villeurbane Cedex, France*
[2]*Center for Photon Information Processing and Graduate School of Information and Communications, Inha University, Incheon 402-751, Republic of Korea*
[3]*Laboratoire des Verres et Ceramiques, UMR-CNRS 6512, Universite de Rennes 1, Campus de Beaulieu, 35042 Rennes Cedex, France*
(Received 19 May 2006; revised manuscript received 16 September 2006; published 6 November 2006)

Both radiative and nonradiative relaxation rates for a series of rare-earth ions doped 20Ge-5Ga-10Sb-65S (GeGaSbS) sulfide (chalcogenide) glasses have been determined. Temperature-dependent lifetimes were carried out for various excited levels of the sample. Radiative decay rates were derived by using the Judd-Ofelt approach. Nonradiative decay rates are evaluated by comparing the inversion of measured lifetimes with the calculated radiative decay rates. We have found that the multiphonon relaxation rates should be a predominant decay mechanism among the excited states if the energy gap to the next lower level is smaller than 2500 cm^{-1}, and the decay mechanism can be determined using the semiempirical "energy-gap law." For an energy gap larger than 2500 cm^{-1}, additional nonradiative decay processes become dominant over the multiphonon decay. Additional nonradiative decay processes have been quantitatively identified with the diffusion-limited relaxation calculations.

DOI: 10.1103/PhysRevB.74.184103 PACS number(s): 61.43.Fs, 67.55.Lf, 63.20.Kr

I. INTRODUCTION

Erbium-doped fiber amplifiers (EDFAs) have been widely used in fiber-optic communications networks because they provide the capabilities of amplification in the third telecommunication window around 1.55 μm. Particularly, Er^{3+} doped aluminosilicate glasses have attracted more attention due to large gain in bandwidth and better performances compared with other types of inorganic materials in terms of stability and connectivity to single-mode optical fibers. To increase the data transmission capacity in telecommunications networks for different wavelengths outside of silica's low-loss window, different rare-earth dopants in several host materials have been proposed in literature. Recently, Tm^{3+} emitting at 1.48 μm fluorescence line by utilizing $^3H_4 \rightarrow {}^3F_4$ transition[1,2] has received attention for the S and S^+ amplification bands. Pr^{3+} doped fluoride glasses[3,4] emitting at 1.31 μm for $^1G_4 \rightarrow {}^3H_5$ transition have been demonstrated for an optical gain of up to 30 dB. The transitions of $(^6F_{11/2}+{}^6H_{9/2}) \rightarrow {}^6H_{15/2}$ in Dy^{3+} also provides a 1.31 μm emission line with a large emission cross section.[5] However, these transitions suffer from large multiphonon relaxation that degrades the efficiency of the radiative emission. The studies of lower phonon energy glass hosts, therefore, are becoming of prime importance for these optical amplifier applications.

Within this aim, sulfide glasses are considered as a potential host material for rare-earth ions due to their lower phonon energy (350 cm^{-1}), which results in lower multiphonon relaxation rates. Owing to these features, optical properties of rare-earth ions doped in the sulfide glasses have been studied for over the past decade.[6–10] However, in sulfide glasses, both radiative and nonradiative relaxation rates have not been well studied. The experimental data of quantum efficiency for many radiative transitions is less than that of the theoretical calculations. This may be because the nonradiative relaxation rate is much larger than the predicted one based on quenching effects.

In this paper, we present both radiative and nonradiative relaxation rates investigated through a series of rare-earth ions doped in GeGaSbS chalcogenide glasses. The work in this paper is divided into two main parts: (i) low concentration of rare-earths dopant is used to reduce the quenching effects, total nonradiative rate attributes to the multiphonon relaxation rate if the energy gap $\Delta E < 2500$ cm^{-1}; (ii) for the energy gap $\Delta E > 2500$ cm^{-1}, some other nonradiative decay processes, which are not consistent with the exponential energy-gap law, become dominant over multiphonon decay. This mechanism is characterized by the diffusion-limited relaxation process. These results are compared with other recent works and reach a new conclusion in the energy-gap law for GeGaSbS chalcogenide glass.

II. MULTIPHONON ENERGY-GAP LAW

For the first main part, the multiphonon relaxation rates for various rare-earth doped GeGaSbS glasses are evaluated with an energy gap varying from 1400 cm^{-1} to 2500 cm^{-1}, which is relevant for four to eight phonons. One signature to distinguish the multiphonon process from the total nonradiative rate is the characteristic temperature dependence of the glasses. Although phonons with different energies can be involved in the transitions, in general the process requires the fewest number of phonons. Thus, it usually depends only on the maximum phonon energy of the host.[11] The multiphonon rate in this case is a predominant decay mechanism and much larger than some other nonradiative rates. Thereby, it might be considered as the total nonradiative decay rate for transitions.

A. Principle

1. Radiative relaxation

The Judd-Ofelt approaches[12,13] are used for the radiative relaxation rate determinations. These empirical approximations are widely applied to calculate $4f$ transition intensities of rare-earth ions doped in various hosts. Its application requires the computation of three Judd-Ofelt parameters Ω_i $(i=2,4,6)$ by a fitting procedure of experimental data normally obtained from ground state absorption. These three parameters are then used to calculate the line strengths of electric and magnetic dipoles transitions (S_{ed}, S_{md}), oscillator strength f between two states leading to the values of spontaneous emission probabilities, radiative lifetimes, branching ratios, and quantum efficiency of levels.

Since the Judd-Ofelt parameters are experimentally determined, the emission oscillator strength $f(\alpha J;\alpha' J')$ for a transition from an excited level αJ to a lower level $\alpha' J'$ could be expressed by the equation using line strengths of electric and magnetic dipole transitions, S_{ed} $(\alpha J;\alpha' J')$ and S_{md} $(\alpha J;\alpha' J')$, respectively,

$$f(\alpha J,\alpha' J') = \frac{8\pi^2 mc}{3h\lambda(2J+1)n^2}\frac{4\pi\varepsilon_0}{e^2}[\chi_{ed}S_{ed}(\alpha J,\alpha' J') + \chi_{md}S_{md}(\alpha J,\alpha' J')]. \quad (1)$$

The spontaneous emission probability $A(\alpha' J';\alpha J)$ between αJ and $\alpha' J'$, can be identified:

$$A(\alpha' J',\alpha J) = \frac{8\pi^2\nu^2 e^2 n^2}{[4\pi\varepsilon_0]mc^3} f(\alpha J,\alpha' J'), \quad (2)$$

where m and e are the mass and electron charge, respectively, c is the vacuum velocity of light, n is the refractive index, ν is the optical frequency, χ is a local field correction factor that is given by $\chi_{ed}=n(n^2+2)^2/9$ and $\chi_{md}=n^3$ representing the electric and magnetic dipole transitions, respectively. The radiative relaxation rates can finally be shown as

$$W_R(J) = \frac{1}{\tau_R(J)} = \sum_{J'} A(\alpha J,\alpha' J'). \quad (3)$$

2. Multiphonon processes

The analysis of the multiphonon decay process in rare-earth ions, in theory, is obtained by the time-dependent perturbation theory. However, under certain approximations, some parameters can be estimated by using the limit theory to lower order-of-magnitude. This model of multiphonon-based perturbation theory has been developed by Risenberg and Moos[14] and is currently being applied by several investigators. The expression for the energy-gap law[15] of the multiphonon emission rate at 0 K is

$$W(0K) = C\exp(-\alpha\Delta E), \quad (4)$$

where both C and α are positive constants involved in the matrix but not dependent on rare-earth species. The α gives the slope of the $\ln[W_{MR}(\Delta E)]$ dependence. If p is the number of phonons simultaneously emitted in the transition, the integer number of phonons p required to conserve energy in a multiphonon decay between two levels is given by $p=\Delta E/h\omega$.

The perturbation theory shows that the nonradiative rate corresponding to the p phonon decays is terminated by using the factor $(n+1)^p$, where $n=n(T)$ is the Bose-Einstein occupation number and n is written as $n(T)=(e^{\hbar\omega/kT}-1)^{-1}$. We can then show the multiphonon emission rate W_{MR} of an excited state by the following equation:

$$W_{MR}(\Delta E,T) = W_{MR}(\Delta E,0K)[n(T)+1]^p, \quad (5)$$

where the first part of the right-hand side determines the multiphonon rate at 0 K, while the second determines the strength of stimulation of the nonradiative transition by the vibration of lattice ions at temperatures higher than 0 K. At higher temperatures, the second term of Eq. (5) is also a function of the energy gap. Thus, Eq. (5) can be described by the following equation:[16]

$$W_{MR}(T) = C\exp(-\alpha'\Delta E), \quad (6)$$

where

$$\alpha' \equiv \alpha - \frac{\ln(1+n)}{\hbar\omega}. \quad (7)$$

According to Eqs. (6) and (7), the multiphonon rate is still an exponential function with energy gap at higher temperatures, but with the reduced logarithmic slope α'.

3. Total decay rate

The total decay rate W_{Tot} is given by the sum of radiative W_{rad} and nonradiative rate W_{Nrad}. The inversion of the measured lifetime and the radiative one represent respectively the total and the radiative emission rates of the level. Theoretically, for low concentration and low excited pump power, the energy transfer among rare-earth ions in a host and the upconversion phenomenon might be negligible. Thus it is possible to assume that the nonradiative emission should attribute only to the multiphonon relaxation rate and can be described as

$$1/\tau_{mes} = W_{Tot} = W_{rad} + W_{Nrad} = W_{rad} + W_{MP}. \quad (8)$$

B. Experiment

1. Sample preparation

The glass samples were composed of 20Ge-5Ga-10Sb-65S, and containing 0.1 at % of Dy^{3+}, Pr^{3+}, Ho^{3+}, Tm^{3+}, and Er^{3+}. The samples were prepared by weighing pure elements in a dry glove box. High purity starting powders were prepared. The mixture needs to be purified, distilled, then melted to ensure the minimum requirement of impurities. The mixture was then placed in a fused silica ampoule and pumped under vacuum at 10^{-4} Torr for a few hours. At this stage, the tube is sealed and placed in a rocking furnace, heated to 800 °C at a rate of 1 °C/min. The mixture is cooled down in the air or in the water to room temperature, then annealed at the glass transition temperature for six hours.

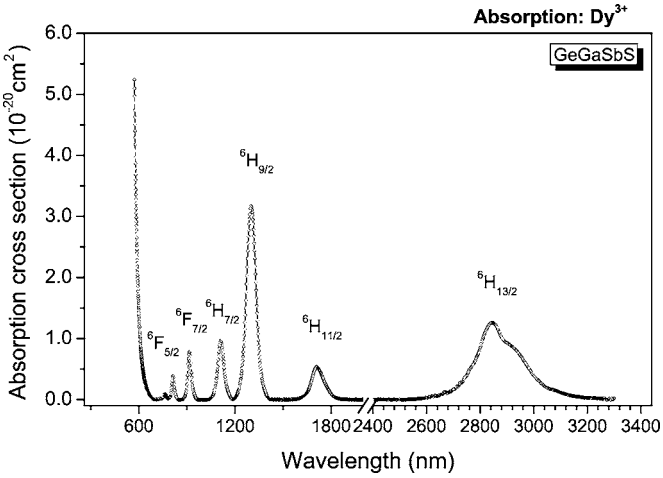

FIG. 1. Absorption cross section of Dy^{3+} in GeGaSbS glass.

2. Absorption and lifetime measurements

Absorption spectra was carried out with a Perkin 950 spectrophotometer on bulk samples for the 0.5 at % of Dy^{3+}, Pr^{3+}, Ho^{3+}, Tm^{3+}, and Er^{3+} doped GeGaSbS glass.

For the luminescence decay measurements, it is well known that in a bulk sample, photons emitted by an ion can be reabsorbed by other ions, and the energy transfer may increase the observed lifetime. This effect is sometimes referred to as the reabsorption phenomenon. The reabsorption phenomenon can be alleviated when the sample is geometrically as small as a fine plate or in a powder form. In our experiments, the samples chosen were in a powder form. Low concentration of 0.1 at % rare-earth doped samples and low pump power of excited laser were used in order to reduce the quenching effects. A selective OPO pulsed laser of Nd^{3+}:YAG was used for the lifetime measurements. The frequency of the pulsed laser ranges from visible to infrared. Spectral decays were detected by photomultiplier R5509, intermedium and high-speed germanium photodiode, cooled by liquid nitrogen. Signals from detectors are recorded with a Lecroy 9410 digital oscilloscope.

Temperature dependence on the emission lifetimes was measured for various temperatures of a cryostat in the range 5–300 K. Emission lifetime measurements for several levels of Dy^{3+}, Ho^{3+}, Pr^{3+}, Tm^{3+}, and Er^{3+} in GeGaSbS glass, where the energy gap is varied from 1400 cm^{-1} to 6500 cm^{-1}, were carried out at various temperatures. Phonon energy of GeGaSbS glass[17] is derived from Raman scattering spectrum, and the main band's peak appeared at around 350 cm^{-1}.

C. Experimental results

1. Judd-Ofelt analyses

Absorption spectra of Dy^{3+}, Pr^{3+}, Ho^{3+}, Tm^{3+}, and Er^{3+} doped GeGaSbS were used for radiative lifetime determinations. Figure 1 shows an example of absorption spectra of Dy^{3+} dopant for the wavelength region from 550 nm to 3440 nm.

In a chalcogenide system, all levels of rare-earth ions with energy values higher than 15 000 cm^{-1} (around 665 nm) were obscured due to the fundamental absorption edge of the host. The losses in this higher spectral region were attributed to the transitions between electronic states of the valence and conduction bands. The measured oscillator strengths of the absorption transitions were derived by integrating each absorption band area. Then, using the calculated matrix elements and at least three or more oscillator strengths, which were calculated from absorption transitions, one can determine the intensity parameters Ω_i $(i=2,4,6)$. The spontaneous emission probabilities and radiative lifetimes of each transition can be finally identified. Table I shows the Judd-Ofelt radiative lifetimes and the energy gap to the next lower level, which was determined from the absorption spectra of Dy^{3+} and Ho^{3+} doped GeGaSbS glass for the energy gap $\Delta E < 2500$ cm^{-1}.

TABLE I. Energy gap and Judd-Ofelt radiative lifetime of excited levels for Dy^{3+} and Ho^{3+} in GeGaSbS.

	Dy^{3+}			Ho^{3+}
Level	$^6F_{5/2}$	$^6F_{11/2}(+^6H_{9/2})$	$^6H_{11/2}$	$^5F_5$
Energy gap (cm^{-1})	1380	1835	2335	2120
Calculated radiative lifetime (μs)	265	380	3350	100

2. Multiphonon rate determination

The radiative transition rate W_{rad} was derived from the inversion of the calculated radiative lifetimes of Table I. Therefore, using Eq. (8), the multiphonon transition rates were calculated by the following:

$$W_{MP}(T) = W_{Tot} - W_{rad} = 1/\tau_{mes}(T) - 1/\tau_{rad}. \quad (9)$$

From Eq. (9), it is possible to plot the multiphonon rate W_{MP} versus the energy gap ΔE at a given temperature T. The empirical energy-gap law of Eq. (4) was then applied to fit the multiphonon relaxation rate W_{mp} versus the energy gap: Both parameters C and α were used to describe the characteristic multiphonon of the hosts that should be determined.

Figures 2–4 show three examples of the temperature-dependent fluorescence decay lifetime (squares) and their best fit curves (solid line) for the $^6F_{5/2}$, $^6F_{11/2}(+^6H_{9/2})$, and $^6H_{11/2}$ levels of Dy^{3+} in GeGaSbS glass. Knowing the measured lifetime at very low temperatures and the radiative one τ_{rad}, the first term W_{MR} $(\Delta E, 0\ K)$ of Eq. (5) can be derived by applying Eq. (9). Taking $n(T)=(e^{\hbar\omega/kT}-1)^{-1}$ and number of phonons $p=\Delta E/\hbar\omega$ for Eq. (5), the measured temperature-dependent lifetimes are then fitted (Figs. 2–4) when combining Eqs. (5) and (8). These fitting curves may be used to account for the phonon energy $\hbar\omega$ and energy gap ΔE (see the inset of Figs. 2–4). Results were compared to the phonon energy values which were obtained from Raman scattering spectra in Ref. 17.

The best fit curve in Fig. 2 is obtained for 4-phonon process with the phonon energy $\hbar\omega=350$ cm^{-1}. Figure 3 shows the best fit curve for 5-phonon process with $\hbar\omega=370$ cm^{-1}. Figure 4 shows the best fit curve for the observed lifetime

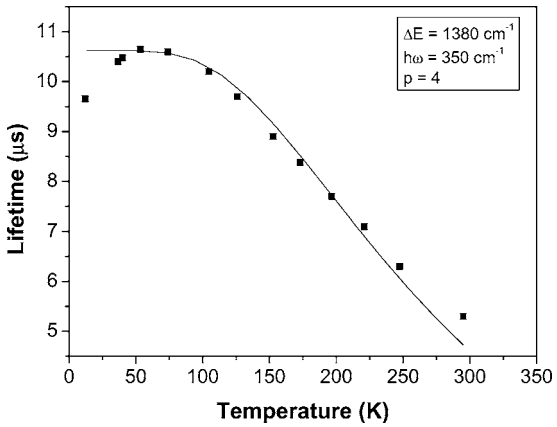

FIG. 2. Experimental temperature dependence of the $^6F_{5/2}$ emission lifetimes of Dy^{3+} doped GeGaSbS and its fitting curve.

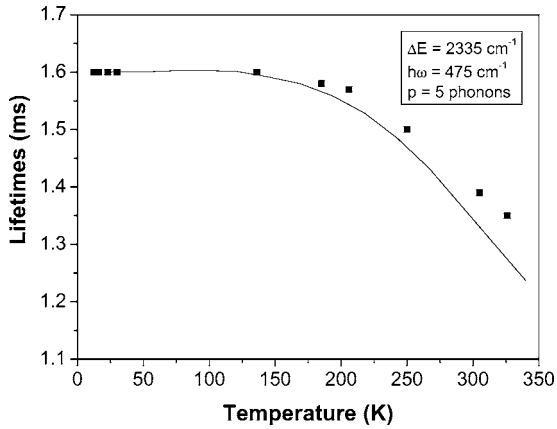

FIG. 4. Experimental temperature dependence of the $^6H_{11/2}$ emission lifetimes of Dy^{3+} doped GeGaSbS and its fitting curve.

measurements, when the number of stimulated phonons is $p=5$ and the phonon energy is $\hbar\omega=475$ cm^{-1}. The calculated phonon energy values at $\hbar\omega=350$ cm^{-1} and 375 cm^{-1} obtained from Figs. 2 and 3 are rather in agreement with the maximum peak of Raman spectra and correspond to the breathing mode of the GeS_4 and GaS_4 groups. For the $\hbar\omega=475$ cm^{-1} vibration, this might be structured at S_3Ga-S-GaS_3 vibration modes, which are due to the presence of some -S-S- bonds.[17] The agreement between the measured temperature-dependent lifetimes and their multiphonon theoretical fit curves leads to a conclusion that the multiphonon relaxation process is the main dominant decay mechanism for range of energy gap restricted to $\Delta E<2500$ cm^{-1}. The energy-gap law of Eqs. (4) and (6) can be applied now to account for the total nonradiative rate versus energy gap ΔE for transitions at a given temperature T.

Figure 5 reports the variation of multiphonon relaxation rates W_{MR} for low temperature as a function of the energy gap ΔE to the next lowest level. The best fit curve (solid line) by the empirical "energy-gap law" describes the characteristic multiphonon relaxation rates in chalcogenides glasses over the region of energy gap from 1400 cm^{-1} to 2500 cm^{-1}. The parameters $C=3.8\times10^9$ s^{-1} and $\alpha=6.9\times10^{-3}$ cm are derived from the least-square curve fit of Eq. (4) from the observed data.

III. ADDITION OF OTHER NONRADIATIVE MECHANISM

The addition of other nonradiative transition rates other than the multiphonon relaxation rates for Er^{3+}, Pr^{3+}, and Tm^{3+} doped GeGaSbS glass is described in this section. This is the case which usually occurs at the range of energy gap $\Delta E>2500$ cm^{-1} (number of phonons emitted in transitions is larger than eight phonons) in a sulfide system. The behavior of the measured lifetime is theoretically related to phonon relaxation processes and characterized by a smooth change with temperature. On the contrary, the results of lifetime measurements present here show an abrupt decrease of lifetime at low temperatures and a slight change at higher temperatures. Similar results were also obtained in our recent work in Ref. 18 for Tm^{3+} doped GeGaSbS glass. These behaviors are interpreted by the diffusion-limited relaxation phenomenon in Ref. 19 and rather similar to that of $Eu(PO_3)_3$ with Cr impurities[20] and of Tb:$Y_3Al_5O_{12}$ crystals with Si and Ca impurities.[21] The energy migration and the direct energy transfer to acceptor ions were investigated in

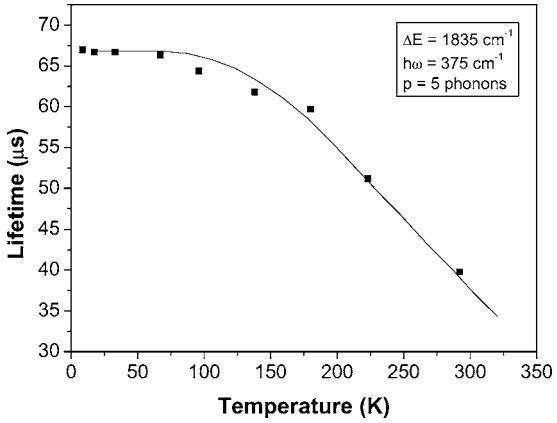

FIG. 3. Experimental temperature dependence of the $^6F_{11/2}$ ($+^6H_{9/2}$) emission lifetimes of Dy^{3+} doped GeGaSbS and its fitting curve.

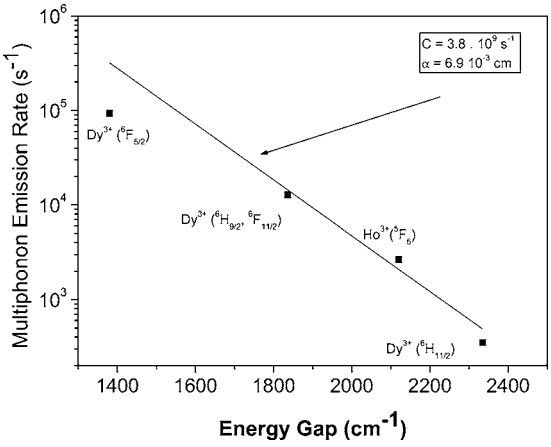

FIG. 5. Multiphonon emission rates of 0.05% Dy^{3+} and Ho^{3+} in GeGaSbS at 10 K as a function of the energy gap.

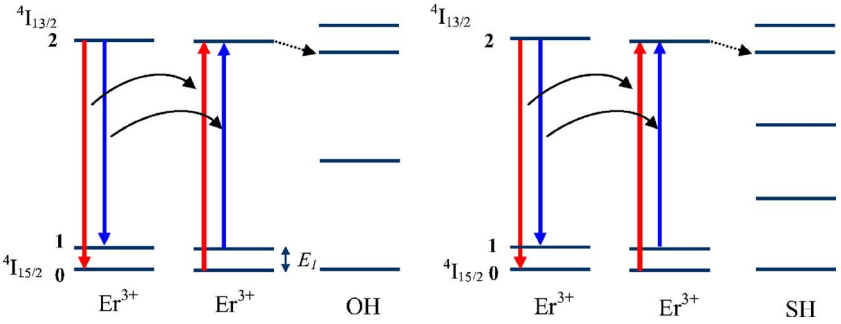

FIG. 6. (Color online) Er^{3+}: $^4I_{13/2}$ energy transfer diagram using diffusion-limited relaxation process.

these references, where the excited Tb^{3+}, Eu^{3+} ions form the donor system and the Si, Ca, and Cr impurities act as energy acceptors. This type of study was continued for theoretical development in the random distribution of acceptor ions in Refs. 22–24 which acted in the host as traps for the optical excitation of Nd^{3+} doped PrF_3 crystals. The donor-acceptor energy transfers here were studied over a wide range of acceptor concentrations for low and high temperature. The theoretical developments of donor fluorescence in the diffusion limit of Ref. 22 have been experimentally improved in Refs. 25 and 26. In this given paper, theoretical best fit curve of the temperature-dependent lifetime using the diffusion limit theory will be displayed and carefully discussed.

A. Diffusion-limited relaxation principle

For the diffusion-limited analysis, the acceptor concentration is considered much lower than the donors and only a small fraction of donor-acceptor transfer probability is being treated as compared to a donor-donor one. Consequently, the donor decay is mainly driven by the intrinsic relaxation and by diffusion-limited relaxation to acceptors. Note that the rates of energy migration of the donors systems and the diffusion by donor-acceptor energy transfer are slow for low donor concentration condition, but still comparable to the intrinsic decay rate. The effective lifetime τ is described by the following:[27,28]

$$\frac{1}{\tau} = \frac{1}{\tau_R} + \frac{1}{\tau_D}, \tag{10}$$

where $1/\tau_D$ is the decay rate due to diffusion relaxation.

In sulfide glasses, energy transfers to a vibrational impurity of OH and SH is one of the main reasons that lead to the quenching of fluorescence lifetime of the excited states. Previous studies have shown, for example, that $Pr:{}^1G_4$ lifetime in a Ge-based sulfide glass is decreased with increasing the concentration of either OH (Refs. 29 and 30) or SH.[31] Some other higher energy vibrations such as a metal-oxide bond Ge-O may be presented, but they do not seem to correlate with a decreased value in the $Pr:{}^1G_4$ lifetime.[31] In this paper, to investigate the diffusion-limited relaxation process under the influence of impurities, we assume that the presence of a likely small level of OH or SH impurities are the acceptors and the rare-earth doped GeGaSbS glasses are the donors. Schematic diagrams of Fig. 6 present detailed examples of energy transfer from $Er^{3+}:{}^4I_{13/2}$ level to the impurity of OH and SH.

The behavior of the diffusion-limited relaxation process versus temperature is related to the diffusion coefficient D. In this condition, D is taken into account by Ref. 19 and written by

$$D \propto \frac{1 + Be^{-E_1/k_BT}}{1 + \frac{g_1}{g_0}e^{-E_1/k_BT}}, \tag{11}$$

where g_i $(i=0,1)$ is the rare-earth ion's Stark sublevel degeneracy and E_1 is the energy of the sublevel 1 of the ground manifolds.

Figure 6 describes two processes of the energy migration between Er^{3+} ion and Er^{3+} ion and their diffusion-limited procedures to a vibrational impurity. The energy migrations of the $Er^{3+}:{}^4I_{11/2}$ and $^4I_{13/2}$ levels is assumed to migrate from ion to ion until they arrive in a neighborhood of an impurity (OH, SH) that absorbs them and then decays in a nonradiative way. It needs to be mentioned that, when the temperature increases, the available resonant transition is not only between $(2\rightarrow 0, 0\rightarrow 2)$ but also $(2\rightarrow 1, 1\rightarrow 2)$ transitions. Considering Eqs. (10) and (11) and under some approximations in Ref. 19 the decay time τ becomes

$$\tau = \left[\left(A \frac{1 + Be^{-E_1/k_BT}}{1 + \frac{g_1}{g_0}e^{-E_1/k_BT}} \right)^{3/4} + \frac{1}{\tau_R} \right]^{-1}, \tag{12}$$

where B is the square of the ratio of the two oscillator strengths between two sublevels and their degeneracies. A is a suitable dimension constant taking into account the diffusion coefficient D.

B. Radiative rate determination

Similarly, the Judd-Ofelt model is applied for the radiative rate calculations of Er^{3+}, Pr^{3+}, and Tm^{3+} in GeGaSbS glass. Note that, both Er^{3+} and Tm^{3+} ions possess several levels with the energy gap to the next lower level $\Delta E > 2500\ cm^{-1}$. Table II presents the energy gap values of each level, measured lifetimes of 0.1 at % of Er^{3+}, Tm^{3+} doped GeGaSbS glass for low temperature (10 K) and their Judd-Ofelt calculated ones.

Normally, the lifetime of an excited state is totally radiative if there are ten or more phonons which are required to make the transition to the next lower level. The measured lifetime τ_m should be equal to radiative lifetimes τ_R without any uncertainty of experiments and calculations. On the con-

TABLE II. Calculated and measured lifetimes and the energy gap of the excited levels for rare-earth ions in GeGaSbS glass.

Level	Tm^{3+}			Er^{3+}	
	$^3H_4$	$^3H_5$	$^3F_4$	$^4I_{11/2}$	$^4I_{13/2}$
Energy gap (cm^{-1})	4230	2410	5845	3665	6500
Calculated radiative lifetime (ms)	*0.120*	*0.65*	*0.85*	*1.50*	*1.85*
Low temperature measured lifetime (ms)	0.155	0.76	1.30	1.60	2.90

trary, Table II presents an inconsistency between the experimental results and their theoretical calculations. The low temperature measured lifetimes of the excited states are much larger than the calculated ones using Judd-Ofelt analysis.

Previous experiments indicate that this mentioned discrepancy is real for several rare-earth doped sulfide glasses. It has been observed in many cases that the Judd-Ofelt approach could not be applied for the radiative relaxation calculation. A similar phenomenon also occurred in the Er^{3+}, Tm^{3+}, Ho^{3+}, and Yb^{3+} ions doped Ge-Ga-S glasses with the addition of alkali halides in the matrix host.[32] In addition, the negative Ω_2 parameters sometimes appeared in the Pr^{3+} or Ho^{3+} ion-doped chalcogenides glasses.[33,34] The quantum efficiency for the Pr^{3+}:$^1G_4$ level is measured independently using a technique that does not rely simply on Judd-Ofelt calculations. In the case of the Dy^{3+}:$^6H_{13/2}$, the calculated radiative rate does not rely directly on a Judd-Ofelt calculation, but is rather derived from the reciprocity between ground state absorption and emission to the ground state.[34]

To understand the physical origin of the above mentioned discrepancies, some hypotheses were proposed in the literature to explain. A hypothesis about the existence of a "local" refractive index given by Refs. 32, 33, and 35 suggests that there might be a different "local" refractive index of local environments around rare-earth ions compared to the refractive index which is experimentally measured from the overall of the hosts. The uncertainty of refractive index determination processes may lead to the difference in spontaneous emission probability calculations that result in the inaccuracy in calculating the radiative rates.

Another possible mechanism for this uncertainty of the radiative rate evaluations was recently presented in Refs. 18 and 36, that a part of rare-earth dopant is treated in a second site with a local environment different from that of the main chalcogenide sites. This means only a "small number" of ions are treated in a chalcogenide site (no extrinsic impurities). Therefore, the absorption cross-section values using the Judd-Ofelt calculation in a chalcogenide site might be smaller than the ones which were determined from the absorption measurements. Experiments in Ref. 36 reveal that the excitation and absorption spectra present different forms due to the influence of small levels of impurities such as oxide, which provides a second site of rare-earth dopants. The rare-earth ions in this second oxide site can constitute up to approximately one third of the total number of ions doping, experience a higher-phonon-energy environment than chalcogenides glasses and cannot provide a gain for transition used in an optical-fiber amplifier. This indicates that the existence of a second site with a local environment different from that of the chalcogenide host can make it inaccurate for the "local" refractive index and/ or the "real" absorption cross-section determinations, and leads to the uncertainty in the radiative rate calculations. Nevertheless, to reevaluate these "local" refractive indexes or the "real" cross sections of transitions, the hypotheses mentioned above indicate that, using a common approximation of low concentration of rare-earth ions with the large energy gap values of excited levels in sulfide glasses, radiative lifetimes of excited states can be directly derived from the lifetime values at very low measured temperature as the energy transfer and migration of ions between levels are ignored. Taken together, this leads to a conclusion that for a rare earth such as Er^{3+} and Tm^{3+} doped GeGaSbS glass that possesses several levels with the energy gap $\Delta E > 2500\ cm^{-1}$, the radiative rates would be directly derived from the measurements at low temperatures rather than from the theoretical calculations.

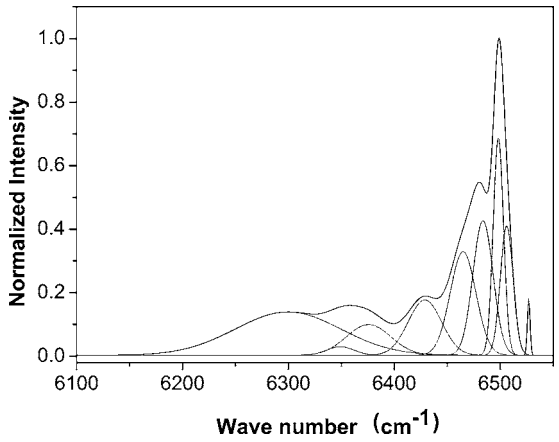

FIG. 7. Emission spectra at 1.5 K permitted to obtain the Stark levels of the Er^{3+}:$^4I_{15/2}$ manifold in sulfide glasses.

C. Experimental results and their theoretical simulations

Equation (12) applies Tm^{3+} and Er^{3+} doped GeGaSbS glass to fit the experimental lifetimes. Radiative lifetimes τ_R in Eq. (12) are taken from the lifetime measurement at low temperatures (see Table II). For theoretical simulations of the diffusion-limited relaxation process, it is necessary to identify the two parameters B and E_1 of Eq. (12). A detailed example for the interpretation of Eq. (12) is presented in the case of the Er^{3+}:$^4I_{13/2}$ level. The sublevel 0 and 1 positions of the $^4I_{15/2}$ manifolds in Fig. 6 are deduced from the emission measurements at low temperatures for the $^4I_{13/2} \rightarrow {}^4I_{15/2}$ transitions. Figure 7 shows the emission spectra for $^4I_{13/2} \rightarrow {}^4I_{15/2}$ transition of Er^{3+} in GeGaSbS glass at low temperatures.

The systematic determination of Stark splitting was derived by using the resonant fluorescence line narrowing (RFLN) data in Ref. 37. Table III presents the $^4I_{15/2}$ Stark positions. Then, from Fig. 7 and Table III, the ratio B and

TABLE III. Stark level positions of Er^{3+}:$^4I_{15/2}$ manifold.

Sublevels	Sublevel energy (cm^{-1})
0	0
1	11.6
2	30.5
3	45.4
4	81.8
5	139.4
6	172.9
7	220.5

energy E_1 of the sublevel 1 can be determined.

Figures 8 and 9 show two examples of the experimental lifetime results of the Er^{3+}:$^4I_{13/2}$ and $^4I_{11/2}$ levels (squares) and their best fits (solid line) using the calculated B and E_1 parameters obtained from the RFLN experiments.

IV. DISCUSSION

In sulfide glasses, the parameters for the multiphonon rates originally obtained in Ref. 38, where Reisfeld presents a review of radiative and nonradiative properties of rare earth in amorphous media. The multiphonon relaxation parameters for LaGaS glass were evaluated in that paper and were widely quoted. However, the energy-gap law presented seems to be anomalous compared to other glasses. Recently, new derived parameters for the multiphonon rates have been inferred by Quimby[16] in GeGaAsS sulfide glasses with an electron-phonon coupling parameter $\varepsilon=0.058$, which is more in line with other glasses than the accepted value of $\varepsilon=0.36$ in Ref. 38. The existence of some other nonradiative processes, which reduces the fluorescence lifetime, has been assumed in the GeGaAsS sulfide glass. However, this additional quenching mechanism is still able to account for an exponential function with energy gap of Eq. (6) at temperatures higher than 0 K. The fit of the curve using this function corresponds to a very different set of multiphonon parameters C and α. To account for this quenching process, the

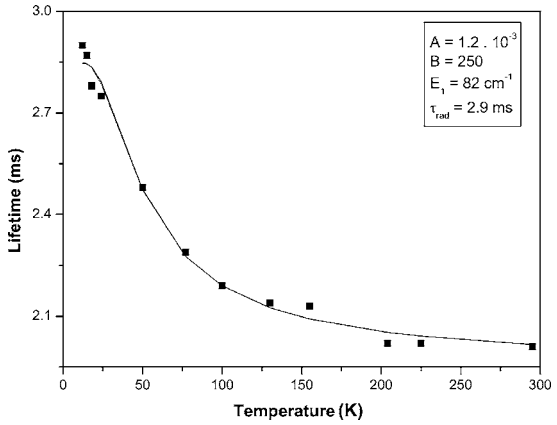

FIG. 8. Er^{3+}:$^4I_{13/2}$ lifetimes versus temperature and its fit curve.

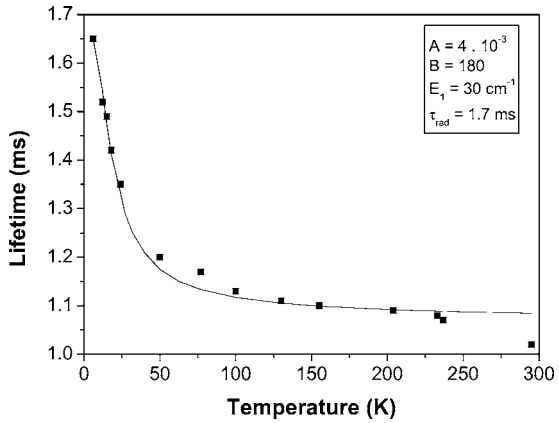

FIG. 9. Er^{3+}:$^4I_{11/2}$ lifetimes versus temperature and its fit curve.

higher phonon energy of vibration modes than the value of the maximum peak of Raman spectra might be involved in the transitions. Several possibilities have been proposed to explain this observation. The nature of this additional decay process is not known for certain, but it is likely due to quenching by vibrational impurities of OH and SH in this sulfide glass.

Within the above mentioned respects, the nonradiative decay rates for various rare-earth ions for the whole range of energy gap ΔE from 1200 cm^{-1} to 6500 cm^{-1} are investigated in our GeGaSbS chalcogenide glass. The parameters C and α for the multiphonon rates are derived and compared with other glass compositions. The total decay rate W_{Tot} from Eq. (8) can be described now by the following:

$$1/\tau_{mes} = W_{Tot} = W_{rad} + W_{Nrad} = W_{rad} + (W_{MP} + W_{other}), \tag{13}$$

where the nonradiative W_{Nrad} in turn has contributions from the multiphonon relaxation rate W_{MP} and possibly other additional nonradiative processes W_{other}. Here, we propose that this quenching mechanism W_{other} is due to the temperature-dependent diffusion-limited relaxation process.

The nonradiative transition rates at a given temperature T can then written by

$$W_{Nrad}(T) = (W_{MP} + W_{other}) = W_{Tot} - W_{rad} = 1/\tau_{mes}(T) - 1/\tau_{rad}. \tag{14}$$

At low temperatures, since the energy transfer to impurities W_{other} strongly decreases as the temperature drops down to zero (see Figs. 8 and 9 for two examples of the abrupt increase in $^4I_{11/2}$ and $^4I_{13/2}$ lifetimes at low temperatures), the multiphonon rates in the whole range of energy gap would be now a predominant decay mechanism. The multiphonon relaxation rates versus the energy gap returns now to the results described in Fig. 5 for transition energy gap $\Delta E < 2500$ cm^{-1}. We assume that for low concentration of rare-earth dopant and at low temperatures, the interaction between rare-earth ions and their energy transfer to vibrational impurities may be ignored at very low temperature.

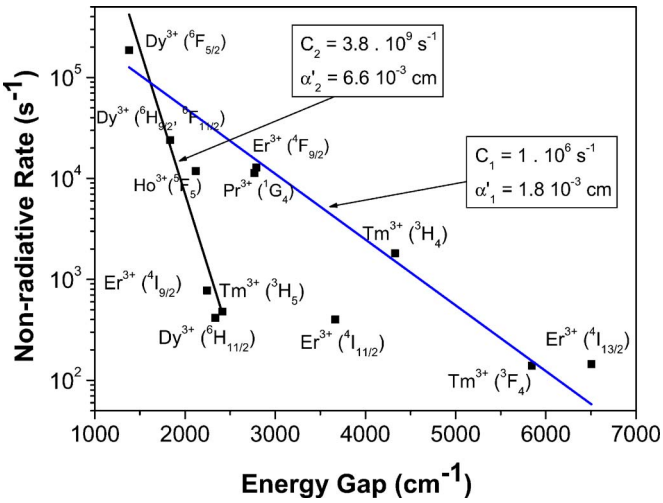

FIG. 10. (Color online) Nonradiative rates for various rare-earths transitions at 300 K as a function of the energy gap.

For the measurements at room temperature, the nonradiative decay rates W_{Nrad} of Eq. (14) are plotted in Fig. 10 as a function of the energy gap between the investigated levels and the next lower level. In Fig. 10, we present the gap laws obtained using Eq. (8), the first one for $\Delta E < 2500$ cm^{-1} and the second one for $\Delta E > 2500$ cm^{-1}. From Fig. 10, it seems possible to fit two exponential nonradiative rate functions with energy gap ΔE using Eq. (8) at high temperatures: The fit curves correspond to the multiphonon parameters $C_1 = 1.0 \times 10^6$ s^{-1}, $\alpha'_1 = 1.8 \times 10^{-3}$ cm and $C_2 = 3.8 \times 10^9$ s^{-1}, $\alpha'_2 = 6.6 \times 10^{-3}$ cm. For $\hbar\omega = 350$ cm^{-1} and $T = 300$ K in Eq. (7), the parameters α can be identified. The multiphonon phenomenological transition parameters C and α of Eq. (4) are depicted in Table IV to compare with other glass compositions.

Table IV shows that the smaller phonon energy $\hbar\omega$ of the GeGaSbS chalcogenide glass presents the smaller values of constant C (3.8×10^9 s^{-1}) with steep slope α ($\alpha = 6.9 \times 10^{-3}$ cm) of the $\ln[W_{MR}(\Delta E)]$ curve, which can result in the lower nonradiative relaxation rates compared to other glasses. However, it must be noted that, the first set of $C_1 = 1.0 \times 10^6$ s^{-1} and $\alpha_1 = 2.1 \times 10^{-3}$ cm ($\Delta E > 2500$ cm^{-1}) in our GeGaSbS chalcogenide glass in Table IV are quite similar to the original values (italic values) obtained by Reisfeld[38] and others.[42–44] In Ref. 16, Quimby assumes the existence of some other unknown quenching mechanism in addition to the multiphonon relaxation rate of GeGaAsS glass. In the case of our GeGaSbS sulfide glass, experimental results in Figs. 8 and 9 reveal that it is impossible to use Eqs. (4) and (6) to examine the behavior of lifetime with temperature using the multiphonon procedure for energy gap of $\Delta E > 2500$ cm^{-1}. Therefore, the roughly fit curve with $C_1 = 1.0 \times 10^6$ s^{-1} and $\alpha'_1 = 1.8 \times 10^{-3}$ cm from Fig. 10 for Eq. (6) cannot be used to characterize the multiphonon rates even for some other additional nonradiative rate versus energy gap at high temperatures. To describe this additional quenching mechanism, the diffusion-limited relaxation process is included and fit curves of measured temperature-dependent lifetimes show theoretically in good agreement with results from experiments. Note that some other possibilities may be included to account for this additional procedure at high temperatures. For example, the up-conversion phenomenon from excited level to the higher levels and/or the transfer of excitation energy to the host glass may occur even at very low concentrations of rare-earth dopant and lead to the increasing nonradiative part of transitions. However, the detail discussions for these quenching processes are beyond the scope of the present work. Further investigation regarding the effects in GeGaSbS glasses can be found in Ref. 33.

TABLE IV. The nonradiative phenomenological transition parameters for different glasses.

Host	C (s^{-1})	α (cm) (10^{-3})	$\hbar\omega$ (cm^{-1})
Borate (Ref. 39)	2.90×10^{12}	3.80	1400
Phosphate (Ref. 40)	5.40×10^{12}	4.70	1200
Silicate (Ref. 40)	1.40×10^{12}	4.70	1100
Germanate (Ref. 38)	3.40×10^{10}	4.90	900
Tellurite (Ref. 38)	6.30×10^{10}	4.70	700
ZBLA (Ref. 39)	1.88×10^{10}	5.77	500
Fluoroberyllate (Ref. 41)	9.00×10^{11}	6.30	500
Ge-Ga-S (Ref. 42)	*8.13×10^5*	*2.83*	*350*
Ge-As-S (Ref. 42)	*2.56×10^6*	*2.95*	*350*
La-Ga(Al)-S (Ref. 38)	*1.00×10^6*	*2.90*	*350*
GeGaAsS (Ref. 16)	(*1.00×10^6*)	*(2.90)*	*(425)*
	3.80×10^9	6.70	425
GeGaSbS (this work)	(*1.00×10^6*)	*(2.1)*	*(350)*
	3.80×10^9	6.90	350

The linear fit of Eq. (6) with $C_2 = 3.8 \times 10^9$ s^{-1} and $\alpha_2 = 6.9 \times 10^{-3}$ cm in Table IV is quite in agreement with those obtained at low temperatures (see Fig. 5) for transitions with $\Delta E < 2500$ cm^{-1}. These latter derived parameters characterize the "true" multiphonon rates in sulfide glasses. The values C and α are similar to those values obtained in Ref. 16 as shown in Table IV. This leads to a conclusion that to fit the "true" multiphonon relaxation rate in sulfide glasses can only be obtained if the range of energy gaps is restricted to $\Delta E < 2500$ cm^{-1}. Otherwise, for the transition of energy gap $\Delta E > 2500$ cm^{-1}, another nonradiative rate has an effect on the total nonradiative rate and this is likely due to the large part of quenching in diffusion-limited relaxation process to the impurities of OH and SH.

V. CONCLUSION

Judd-Ofelt analyses were used to predict the radiative rates of Dy^{3+} and Ho^{3+} doped GeGaSbS glass. The total decay rates were deduced from the inversion of measured lifetime, then the nonradiative decay rates were determined by comparing them with radiative ones. For transition energy gap $\Delta E < 2500$ cm^{-1}, the true multiphonon relaxation rates were evaluated using the well-known semiempirical "energy-gap law." The newly derived multiphonon parameters were found, and results were compared to other glass compositions. These multiphonon parameters are in agreement with the recently obtained values in the literature.

We also found that for rare-earth dopants which possess several levels of energy gaps $\Delta E > 2500\ \mathrm{cm}^{-1}$, such as the Er^{3+} and Tm^{3+} ions doped GeGaSbS glass, the Judd-Ofelt approach presents a poor condition for the radiative rate calculations. The behavior of the measured lifetime versus temperature was not characterized by the multiphonon relaxation processes. Thus, another nonraditive relaxation rate was included and this quenching mechanism can be interpreted by the diffusion-limited relaxation phenomenon to vibrational impurities such as OH or SH. The behavior of lifetime versus temperature was quantitatively determined using the diffusion-limited relaxation calculation. The existence of these additional diffusion-limited rates might be responsible for the inconsistency between the Judd-Ofelt calculated radiative lifetimes and the measured ones at low temperatures. It is necessary to directly measure the fluorescence lifetime rather than rely on the theoretical calculations.

The paper presents our results of the influences of impurities on host materials in a GeGaSbS sulfide system. In this paper, we assume that the vibrational impurities of OH and SH concentrations are low enough in order to find the best fit (theoretical) curve of the temperature dependent lifetime using the diffusion limit theory. In the future, further investigation for the existence of the additional nonradiative component to the decay, and its dependence on OH or SH concentrations content in the glass should be included. These present potential results in identifying the loss mechanism of rare-earth lasers in sulfide glasses.

ACKNOWLEDGMENTS

The authors would like to thank the LVC laboratory, University of Rennes I, France for providing the glass synthesis. This work was supported by the LPCML laboratory, University of Claude Bernard Lyon I, France, and the Creative Research Initiative Program (Center for Photon Information Processing) of MOST and KOSEF, S. Korea.

*Corresponding author. FAX: +82-32-865-0480. Electronic address: bham@inha.ac.kr

[1] F. Roy, A. LeSauze *et al.*, in Optical Amplifiers and their Applications, Stresa, Italy, 2001, PD4-1-PD4-3.
[2] T. Komukai, T. Yamamoto *et al.*, Electron. Lett. **29** (1), 110 (1993).
[3] M. Yamada, T. Kanamori, Y. Ohishi, M. Shimizu, Y. Terunuma, S. Sato, and S. Sudo, IEEE Photonics Technol. Lett. **9** (3), 321 (1997).
[4] T. Whiley, in European Conference on Optical Communications, Florence, Italy, 1994, pp. 939–946.
[5] K. Wei, D. P. Machewirth, J. Wenzel, E. Snitzer, and G. H. Sigel, Opt. Lett. **19** (12), 04 (1994).
[6] R. Reisfeld, Ann. Chim. (Paris) **7**, 147 (1982).
[7] K. Wei, D. P. Machewirth, J. Wenzel, E. Snitzer, and G. H. Sigel, Opt. Lett. **19**, 904 (1994).
[8] J. A. Medeiros Neto, E. R. Taylor, B. N. Samon, J. Wang, D. W. Hewak, R. I. Laming, D. N. Payne, E. Tarbox, P. D. Maton, G. M. Roba, B. E. Kinsman, and R. Hanney, J. Non-Cryst. Solids **184**, 292 (1995).
[9] Y. Ohishi, A. Mori, T. Kanamori, K. Fujiura, and S. Sudo, Appl. Phys. Lett. **65**, 13 (1994).
[10] J. Heo, J. Mater. Sci. Lett. **14**, 1014 (1995).
[11] L. A. Riseberg and M. J. Weber, in *Progress in Optics*, Vol. 14, edited by E. Wold (North-Holland, Amsterdam, 1976).
[12] B. R. Judd, Phys. Rev. **127**, 750 (1962).
[13] G. S. Ofelt, J. Chem. Phys. **37**, 511 (1962).
[14] L. A. Riseberg and H. Moos, Phys. Rev. **174**, 429 (1968).
[15] C. B. Layne, W. H. Lowdermilk, and M. J. Weber, Phys. Rev. B **16**, 10 (1977).
[16] R. S. Quimby and B. G. Aitken, J. Non-Cryst. Solids **320**, 100 (2003).
[17] J. L. Adam, Y. Guimond, A. M. Jurdyc, L. Griscom, J. Mugnier, and B. Jacquier, Proc. SPIE **3280**, 31 (1998).
[18] V. G. Truong, A. M. Jurdyc, B. S. Ham, B. Jacquier, A. Q. Le Quang, J. Leperson, V. Nazabal, and J. L. Adam (unpublished).
[19] F. Cornacchia, L. Palatella, A. Toncelli, M. Toncelli, A. Baraldi, R. Capelletti, E. Cavalli, K. Shimamura, and T. Fukuda, J. Phys. Chem. Solids **63**, 197 (2002).
[20] M. J. Weber, Phys. Rev. B **4**, 2932 (1971), and references therein.
[21] J. P. Van der Ziel, L. Korf, and L. G. Van Uitert, Phys. Rev. B **6**, 615 (1972).
[22] D. L. Huber, Phys. Rev. B **20**, 2307 (1979).
[23] K. K. Ghosh, L. H. Zhao, and D. L. Huber, Phys. Rev. B **25**, 3851 (1982).
[24] D. L. Huber, Phys. Rev. B **26**, 3937 (1982).
[25] K. K. Ghosh, J. Hegarty, and D. L. Huber, Phys. Rev. B **22**, 2837 (1980).
[26] J. Hegarty, D. L. Huber, and W. M. Yen, Phys. Rev. B **23**, 6271 (1981).
[27] M. Yokota and O. Tanimoto, J. Phys. Soc. Jpn. **22** (3), 779 (1967).
[28] P. G. De Gennes, J. Phys. Chem. Solids **7**, 345 (1958).
[29] M. Naftaly, A. Jha, and W. G. Jordan, J. Appl. Phys. **84**, 1800 (1998).
[30] D. R. Simson, A. J. Faber, and H. de Waal, J. Non-Cryst. Solids **185**, 283 (1995).
[31] M. Scheffler, J. Kirchhof, J. Kobelke, K. Schuster, and A. Schwuchow, J. Non-Cryst. Solids **256-257**, 59 (1999).
[32] Y. B. Shin, J. Heo, and H. S. Kim, J. Mater. Res. **16**, 1318 (2001).
[33] V. G. Truong, Doctoral thesis, University of Lyon I, 2004.
[34] R. S. Quimby, K. T. Gahagan, B. G. Aitken, and M. A. Newhouse, Opt. Lett. **20**, 2021 (1995).
[35] A. M. Jurdyc, V. G. Truong, B. Jacquier, V. Nazabal, J. Leperson, and J. L. Adam, in Proc. IWPA, Hanoi, Vietnam, 2004, p. 201.
[36] T. Schweizer, F. Goutaland, E. Martins, D. W. Hewak, and W. S. Brocklesby, J. Opt. Soc. Am. B **18**, 1436 (2001).
[37] L. Bigot, Doctoral thesis, University of Lyon I, 2002.
[38] R. Reisfeld, J. Electrochem. Soc. **131**, 1360 (1984).
[39] R. Reisfeld and C. K. Jorgensen, in *Handbook on the Physics and Chemistry of Rare Earths*, Vol. 9, edited by K. A. Gschneider, Jr. and L. Eyring (North-Holland, Amsterdam, 1987), Chap. 58, p. 1.

[40] R. Reisfeld, in *Spectroscopy of Solid-State Laser-Type Materials*, edited by B. Di Bartolo (Plenum, New York, 1987), pp. 343–396.
[41] C. B. Layne and M. J. Weber, Phys. Rev. B **16**, 3259 (1977).
[42] Y. B. Shin, W. Y. Cho, and J. Heo, J. Non-Cryst. Solids **208**, 29 (1996).
[43] K. Kadono, M. Shojiya, M. Takahashi, H. Higuchi, and Y. Kawamoto, J. Non-Cryst. Solids **259**, 39 (1999).
[44] T. Y. Ivanova, A. A. Man'shina, A. V. Kurochkin, Y. S. Tver'yanovich, and V. B. Smirnov, J. Non-Cryst. Solids **298**, 7 (2002).